

Fabrication of low cost and low impact RH and temperature sensors for the Internet of Environmental-Friendly Things

Aniello Falco ¹, Philipp S. Sackenheim ², Francisco J. Romero ³, Markus Becherer ², Paolo Lugli ¹, José F. Salmerón ³, Almudena Rivadeneyra ^{3,*}

¹ Faculty of Science and Technology, Free University of Bolzano, 39100 Bolzano-Bozen, Italy

² Institute for Nanoelectronics, Technical University of Munich, 80333 Munich, Germany

³ Pervasive Electronics Advanced Research Laboratory (PEARL), Department of Electronics and Computer Technology, University of Granada, 18071 Granada, Spain

*Corresponding author. Tel: +34958248996. E-mail: arivadeneyra@ugr.es

Abstract- Given the increasing number of connected devices as a consequence of the Internet of Things (IoT) revolution, the issue of the removal and recycling of electronics is becoming more and more urgent. In this context, biodegradable electronics is expected to be one of the biggest technological revolutions to tackle this problem. Following this direction, in this work we present the fabrication and characterization of temperature and humidity sensors based on biodegradable materials with the goal of making their removal easier as well as reducing their environmental impact. In particular, these multi-sensing devices were fabricated following a screen-printing process using a carbon-based paste and a conjugated polymer, both on paper and on a water soluble substrate. The results are more than promising and show how with our biodegradable sensors it is possible to obtain a sensitivity of 1 dec/20%RH to moisture content and around 0.04%/°C sensitivity to temperature. It is demonstrated that the simplicity and flexibility of the fabrication approach followed in this work paves the way to a set of new “green” IoT nodes that could be extended to wide range of sensing applications.

Keywords: carbon; humidity; paper; PVA; PEDOT:PSS; screen-printing; temperature

1. Introduction

Sensing technologies are one of the key fields in both consumer electronics and industrial environment. Today we are measuring everything; sensors are in cars, buildings, cell phones, watches, and many other things of our daily life. Thus, this trend towards an ubiquitous sensing has made that the research and development in this field becomes particularly interesting.

Humidity sensors are among the most studied in this area since they play a key role in several areas, such as agriculture, food industry or healthcare (e.g., pharmaceutical & bio-tech

31 fabrication) [1], [2]. Humidity sensors are usually capacitive or resistive and, although there are
32 further variations, they differ from others mainly in their preciseness, time response, size and
33 costs [3]. However, given the circumstances imposed by the new technological applications,
34 further aspects are becoming of special interest for their development, such as flexibility,
35 biocompatibility or easy disposability [4]–[6]. This has led the novel fabrication methods to be
36 focused not only on a highly scalable and economic production of devices, but also on their
37 biodegradability in order to minimize, or even eliminate, their impact on the environment [7].

38 Printed sensors step exactly in this demand, as they allow the fabrication of cost-effective
39 sensors based on fully biodegradable conductive pastes, sensitive materials and substrates [8],
40 [9]. Therefore, several printable and organic materials have been proposed in this direction,
41 such as conjugated polymers [9], graphene-based materials [10]–[12] and carbon-based pastes
42 [13]. In the same way, different flexible substrates have also been used to deposit these materials,
43 including paper [14]–[16] or liquid crystal polymers [17], [18], among others [19], [20].

44 Many of these materials and substrates has been already studied to develop temperature and
45 humidity sensors, however, most of the implementations proposed in the literature resort to
46 non-biodegradable materials to develop some elements of the final devices. For instance, Khan
47 *et al.* presented a printed humidity sensor based on an egg albumin sensitive layer, but using
48 silver electrodes on a PET substrate [21]. This approach was also followed in [22] and [12]
49 using graphene oxide as sensitive layer and, in general, it can be found in many other works
50 with different kind of materials [21], [23], [24]. Alternatively, Alammouz *et al.* proposed a
51 capacitive humidity sensor based on self-assembled graphene oxide sheets on a paper substrate,
52 but with the drawback of using electrodes made of aluminum [25].

53 Within this context, in this work we present the fabrication and characterization of flexible
54 humidity and temperature sensors by means of printing techniques and biodegradable materials
55 (for both electrode and substrate) that are fully compatible with a cost-effective fabrication of
56 eco-friendly devices. For that, a simple screen-printing process was used, demonstrating the
57 feasibility of this approach through the combination of different conductive pastes and
58 substrates. On one hand, we used standard paper as substrate since, in addition to being
59 compatible with printing techniques and providing flexibility, its hydrophilic nature makes it a
60 perfect candidate to act as a sensing material in RH sensors [26]–[28]. On the other hand, poly-
61 vinyl alcohol (PVA) films were also used for this purpose, given that the dielectric and
62 conductive properties of this hygroscopic polymer change when the hydroxyl groups (O-H) of

63 its structure interact with the water molecules [29]. These two substrates were used to print on
64 them different electrodes configurations also using fully biodegradable conductive materials,
65 specifically poly(3,4-ethylenedioxythiophene) polystyrene sulfonate (PEDOT:PSS) and a
66 carbon-based paste. Each possible combination of these two conductive pastes and substrate
67 materials was fabricated and characterized.

68 The manuscript is structured as follows: following this introduction, Section 2 summarizes the
69 materials used for the fabrication of the sensors, together with the methodologies followed for
70 their characterization. Section 3 presents the results of the temperature and humidity sensors
71 fabricated, as well as a hybrid configuration to monitor both temperature and humidity on the
72 same device. Finally, the main conclusions are drawn in Section 4.

73 **2. Experimental Section**

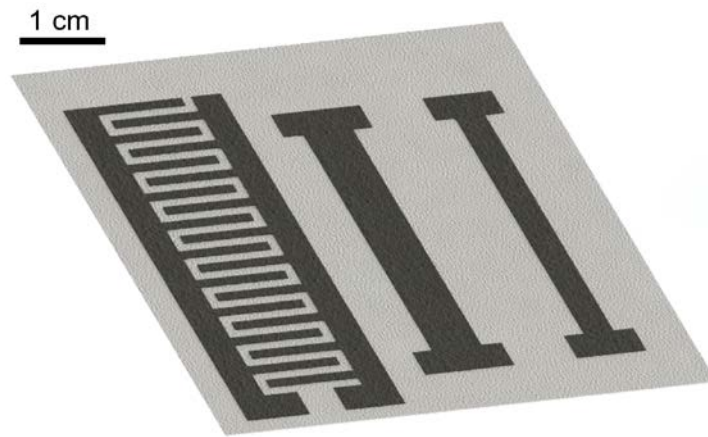
74 **2.1. Materials**

75 Two conductive inks were used for the fabrication of the printed sensors, poly(3,4-
76 ethylenedioxythiophene)-poly(styrenesulfonate) (PEDOT:PSS) and a commercial carbon-
77 based paste, both of them providing flexibility and biodegradability. PEDOT:PSS at a weight
78 content of 1.3 wt.% (viscosity: >14000 mPa.s) was acquired from Sigma Aldrich (St. Louis,
79 MO, USA) [30], while the Loctite ECI 8001 E&C carbon-based paste (viscosity: 6500 mPa.s)
80 was provided by Henkel AG (Düsseldorf, Germany) [31]. These pastes were printed on three
81 different substrates: standard paper (DIN ISO 9706, 80g/m²) [32], polyvinyl alcohol (PVA)
82 films from Wagner Polymertechnik GmbH, and polyethylene terephthalate (PET) foils from
83 DuPont (product name: Melinex® 506, Wilmington, DE, USA) [33]. This latter only for
84 comparison and control since it is not biodegradable.

85 **2.2. Devices Fabrication**

86 A capacitive Interdigitated Electrode (IDE) structure was considered for the RH monitoring
87 devices. Given that the dependence of the dielectric constant of the substrates with respect to
88 the RH, the capacitance of these structures is also subject to the level of RH [34]. The advantage
89 of the IDE layout lays in the simplicity of its geometry, and therefore, its easy application via
90 printing on the flexible substrates [35]. After optimizing the four combination of pastes and
91 substrates by printing lines of several widths, the combination carbon on PVA-L limited the
92 resolution of our patterns with 800 µm as minimal reproducible dimension. The IDE structure
93 used in work (Figure 1) has 10 fingers per electrode with a distance between consecutive fingers

94 and width of 1 mm. These dimensions are large enough to minimize the possible effects on the
95 capacitance as a consequence of the paste spreading over the substrate after the screen-printing
96 process. Moreover, given that the resistivity of both of the conductive pastes used is
97 temperature-dependent [31], [36], we opted for a resistive sensor for the temperature monitoring
98 which consisted of a simple line with a length of 5 cm. In addition, in order study the change in
99 resistance with respect to the temperature (sensitivity and hysteresis) at different average
100 resistances, we tested two different lines widths (3 mm and 5 mm), as it is shown in Figure 1.



101

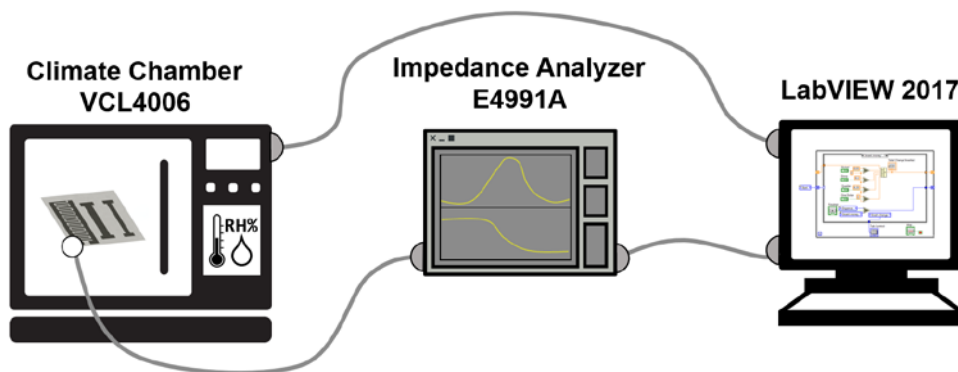
102 **Figure 1.** Left: Capacitive IDE layout. Right: Resistive line layouts with the same length (5 cm) and different
103 widths (5 mm and 3 mm).

104 These layouts were screen-printed with the different pastes on the different substrates with a
105 manual screen-printer (FLAT-DX200, from Siebdruck-Versand, Magdeburg, Germany).
106 Before printing, the PET substrate was washed using deionized water and ethanol with the
107 assistance of ultrasonic treatment in order to remove the impurities on the surface [37].
108 Moreover, pressurized air was applied to the paper substrate with the same purpose, whereas
109 no cleaning process was carried out for the PVA films. No pretreatment was needed to screen
110 printing the pastes on any of the substrates. The mesh used in this work was a 120 Threads per
111 cm (T/cm) polyester mesh with a thickness of 65 μm , a thread diameter of 40 μm and an opening
112 width of 47 μm which, according to the manufacturer, results in a theoretical wet film thickness
113 of $t_{\text{theo}} = 19.5 \mu\text{m}$. After printing, the samples were dried using a UF55 oven (from Memmert,
114 Schwabach, Germany) at 80 $^{\circ}\text{C}$ in order to avoid the degradation of the substrates. We also
115 considered two different curing times, 30 min and 60 min, to evaluate the influence of the drying
116 process in the conductivity of the screen-printed patterns.

117 **2.3. Characterization**

118 The sheet resistance of the conductive layers was measured using a four-point probe head from
119 Jandel (Leighton Buzzard, UK) connected to a source measuring unit (Keysight B2901A,
120 Beaverton, OR, USA). The thickness of the samples was acquired using a DekTak XT contact
121 profilometer (from Bruker Corporation, Billerica, MA, USA).

122 The characterization of the sensors under different environmental conditions (temperature and
123 humidity) was performed using the setup shown in Figure 2. The sensors were connected to an
124 impedance analyzer E4991A using a 42941A impedance probe kit (both from Keysight
125 Technologies, Inc., CA, USA). Afterwards, each connected sensor was placed into a climate
126 chamber VCL4006 (from Vötsch Industrietechnik GmbH, Balingen, Germany) and its
127 impedance was measured from 1 kHz to 10 MHz under different values of temperature and
128 humidity. The whole measurement setup was automatized using LabVIEW 2017 (from
129 National Instruments Corporation, TX, USA).



130

131 **Figure 2.** Characterization setup for humidity and temperature sensors.

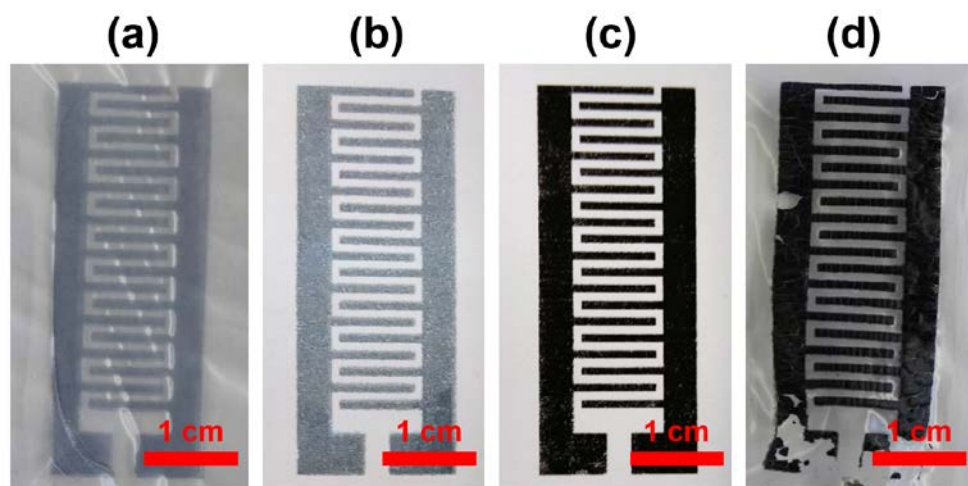
132 The humidity sensors were tested as a function of both varying humidity and temperature.
133 Firstly, the humidity sensors were characterized ranging the relative humidity level from
134 20%RH to 70%RH and vice versa at a temperature of 40 °C. RH was changed in steps of
135 10%RH every 30 min to ensure the uniformity of RH value in the whole chamber's volume.
136 Secondly, both sensors (resistive and capacitive) were characterized as a function of the
137 temperature. For that, it was ranged from 15 °C to 75 °C and vice versa at a fixed 60%RH. In
138 this case, the temperature was varied in steps of 5 °C every 20 min.

139 3. Results and Discussion

140 Throughout this section, we show the results obtained for the characterization of both humidity
141 and temperature sensors fabricated with the biodegradable carbon-based and PEDOT:PSS
142 pastes on both paper and PVA films. The results are also compared with respect to those
143 obtained using PET as substrate of reference.

144 3.1. Physical Characterization

145 All the fully-biodegradable RH sensors fabricated in this work are shown in Figure 3. After
146 visual inspection, it can be clearly observed that all inks were properly transferred to the
147 substrates, except for the carbon-based paste on the PVA substrate (Figure 3d). In that case, the
148 printing of the carbon paste (with a thickness of $10 \pm 1.2 \mu\text{m}$) on the thin PVA substrate ($30 \mu\text{m}$)
149 produces a non-flexible device. Thus, when this device is bent, cracks appear on the whole
150 carbon layer surface. However, this does not happen on the paper substrate, whose surface
151 roughness and greater thickness ($\sim 100 \mu\text{m}$) enhance the adhesion of the carbon-paste (Figure
152 3c). On the contrary, the PEDOT:PSS layer, which is thinner ($2 \pm 0.3 \mu\text{m}$), presents a good
153 adhesion and flexibility on both paper and PVA substrates.



154

155 **Figure 3.** Real view of the screen-printed sensors: (a) PEDOT:PSS on PVA, (b) PEDOT:PSS on paper, (c) carbon-
156 based paste on paper and (d) carbon-based paste on PVA. Scale bars: 1 cm.

157 The sheet resistances of each one of these patterns are presented in Table 1 for the different
158 curing conditions. These values were obtained at ambient conditions, whereas errors were
159 calculated as the standard deviation of five different samples. As seen, any substantial variation
160 was observed when increasing the curing time. These values are also in accordance with respect

161 to the obtained in other works, both for PEDOT:PSS [38]–[40] and for carbon-based pastes
162 [41].

163

164

165

166 **Table 1.** Sheet resistance values for the different pastes and substrates under different curing conditions.

Paste	Substrate	Sheet Resistance (k Ω /sq.)	Sheet Resistance (k Ω /sq.)
		(curing: 30 min at 80 °C)	(curing: 60 min at 80 °C)
Carbon	Paper	3.84 \pm 0.86	3.73 \pm 0.84
	PVA	3.89 \pm 0.93	3.85 \pm 0.93
PEDOT:PSS	Paper	1.20 \pm 0.13	1.09 \pm 0.08
	PVA	1.21 \pm 0.16	1.09 \pm 0.09

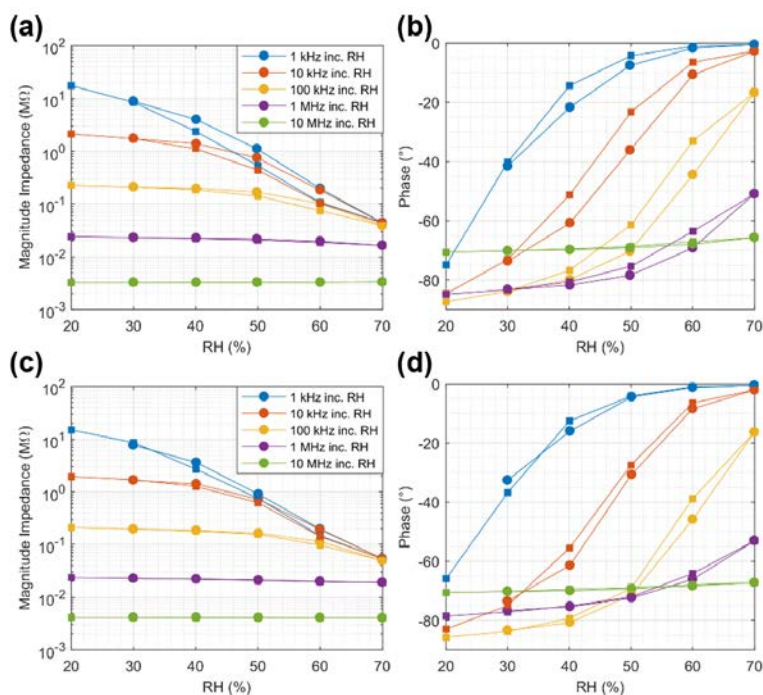
167

168 3.2. Characterization in relative humidity

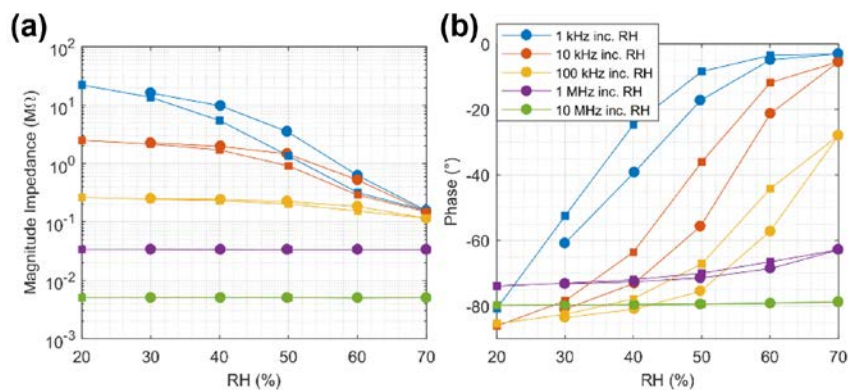
169 Firstly, we characterized the impedance of the capacitive humidity sensors as a function of the
170 RH. The results of these experiments are shown in Figure 4 for the PEDOT:PSS IDEs and in
171 Figure 5 for the carbon-based ones. Reference calibration curves on PET can be found in
172 supplementary Figure S1 and Figure S2, respectively.

173 On one side, the impedance of both carbon paste and PEDOT:PSS on PET shows no
174 dependence on RH at any of the studied frequencies. In that case, the modulus and phase of the
175 impedance remain almost constant for the different values of RH and decrease as the frequency
176 increases. In the case of the phase, the decrease is less abrupt and, as capacitive structure, it is
177 around -90° [42]. On the other side, it can be seen in Figure 4 that the same capacitive structure
178 behaves differently on the other substrates. At low RH values, both on paper and PVA, the
179 PEDOT:PSS structures behave as a capacitor (phase close to -90°). However, as RH increases,
180 the phase decreases indicating an increase in the capacitor dissipation factor. This phenomenon
181 can be related to an increase in the polymer conductivity as a consequence of the moisture
182 accumulation on the sensing layer (i.e., the substrate), hence causing the apparition of electrical

183 paths between electrodes. As a result of this, at high RH levels the devices start to behave more
184 like a resistor (phase closer to 0°) than like a capacitor [42].



185
186 **Figure 4.** Impedance of the PEDOT:PSS IDEs on paper (magnitude: (a), phase: (b)) and on PVA (magnitude: (c),
187 phase: (d)).



188
189 **Figure 5.** Impedance of the carbon IDEs on paper (magnitude: (a), phase: (b)).

190
191 Moreover, this behavior is similar to that obtained for the carbon-based IDEs on paper, as
192 shown in Figure 5, which supports the theory that dependence with respect to the RH arises
193 mainly from the properties of the sensing layer [43]. Finally, Figure S3 shows the results
194 obtained for the the carbon- based paste on PVA, which demonstrates the non-viability of this
195 combination for screen-printing (as it was shown in Section 3.1).

196 In general, in all cases a sensitivity as high as 1 dec/20%RH can be reproducibly achieved. In
 197 all the analyzed combination of materials, the impedance changes abruptly from 20 to 60%RH
 198 and then its responses is saturated. This behaviour is particularly significant up to 100 kHz. At
 199 low RH values, the devices are mainly capacitive (phase $<80^\circ$) and when RH increases, their
 200 phases decrease, achieving phases above -10° at 60%RH (mainly resistive). However, there are
 201 differences related to the hysteresis of the sensors, the lowest value (below 3%) is found for
 202 PEDOT:PSS IDES on PVA, followed by PEDOT:PSS on paper (5%). In general, as it can be
 203 seen in Figure 4 and Figure 5, the paper substrate results in a higher hysteresis than the case of
 204 the PVA substrate.

205 Regarding the dynamic response of the sensors, we define the response time as $t = \tau$, which
 206 corresponds to the 63% of the maximum value of magnitude reached at equilibrium (for every
 207 increasing step of RH). Table 2 summarizes the response time for each one of the analysed
 208 devices.

209 **Table 2.** Time response for RH

Substrate	Time response of PEDOT:PSS IDES (min)	Time response of Carbon IDES (min)
PVA	5.8	6.5
Paper	4.6	4.8

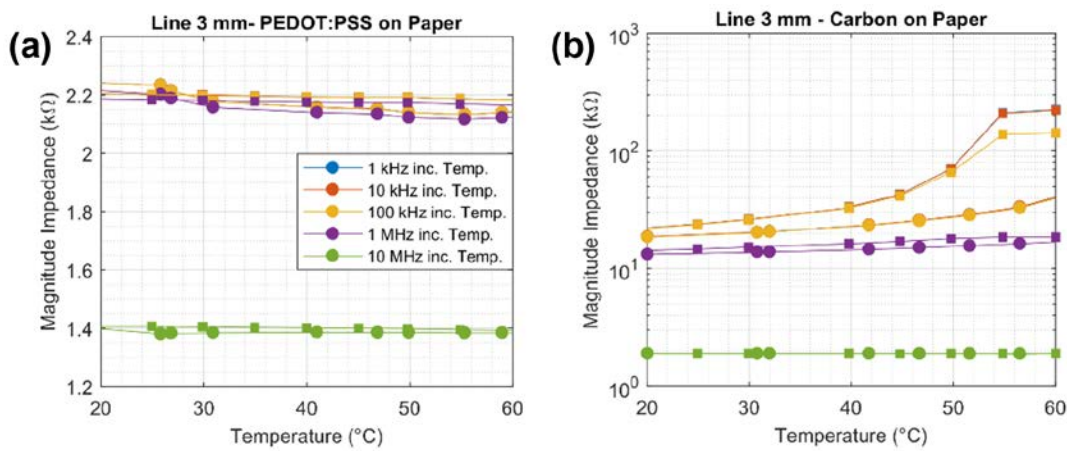
210

211 **3.3. Characterization in Temperature**

212 As it was already introduced, the resistivity of both PEDOT:PSS and carbon-based pastes used
 213 in this work is temperature-dependent. In the case of the PEDOT:PSS, it exhibits a Negative
 214 Temperature Coefficient (NTC) [36], [44], whereas the Loctite ECI 8001 E&C paste is a
 215 Positive Temperature Coefficient (PTC) ink [31]. On this basis, we characterized the impedance
 216 of the resistive patterns as a function of the temperature on a paper substrate. Looking at the
 217 behavior of single lines on paper using the same conductive materials (Fig. 6), we found that
 218 PEDOT:PSS showed a relative linear response at 1 kHz in the temperature range analyzed, as
 219 it was also demonstrated in other works [45], [46]. These sensors exhibited a sensitivity of
 220 around $0.04\%/^\circ\text{C}$ and $0.03\%/^\circ\text{C}$ (considering the relative resistance change as output variable)
 221 for the 3 mm and 5 mm lines width, respectively. Contrary to this, carbon lines exhibited a quite
 222 linear response at low temperatures, but surpassing the $\sim 50^\circ\text{C}$ their resistivity presented a sharp
 223 step response. It can be also seen that the response of the carbon-based paste presents a higher

224 hysteresis than the PEDOT:PSS paste. These two effect are in accordance with the data
 225 provided by the manufacturer [31].

226 For these structures, the sensitivity can be estimated as 3%/°C, which is significantly high
 227 enough to be easy detectable with any low-cost measurement equipment. Furthermore, the
 228 results obtained for the lines with 5 mm of width (supplementary Figure S4) showed that, while
 229 the temperature response and hysteresis of the PEDOT:PSS patterns does not suffer significant
 230 changes, the hysteresis presented by the carbon-based paste is reduced as a consequence of the
 231 overall reduction of the pattern resistance.



232 **Figure 6.** Impedance vs. temperature at different working frequencies of lines on paper made of PEDOT:PSS
 233 and Carbon with width of 3 mm.

234
 235 Regarding the dynamic response of the sensors and following the same definition as the one
 236 employed for RH, Table 3 depicts the response time for each sensor characterized.

237 **Table 3.** Time response for Temperature

Substrate	Time response of PEDOT:PSS IDES (min)	Time response of Carbon IDES (min)
PVA	3.9	3.3
Paper	4.5	3.8

238
 239 **3.4. Comparison with similar sensors in the literature**
 240 In this section, we compare the sensors proposed in this work with other fully biodegradable
 241 sensors presented in the literature. The comparison was made in terms of type of sensor,
 242 materials, fabrication process, area and sensitivity to the variable to monitor (temperature or

243 humidity), as presented in Table 4. In recent years, novel approaches on carbon nanotubes
 244 (CNTs) in their various forms, single-walled and multi-walled (SWCNTs, MWCNTs), are
 245 positioning this material among the most promising materials for the development of
 246 biodegradable sensors [47]. For instance, Liakos *et al.* [48] and Zhu *et al.* [49] used this
 247 conductive organic material to fabricate humidity sensors on different biodegradable substrates,
 248 achieving a quite similar sensitivity to humidity changes. However, although these sensors also
 249 provide interesting features such as flexibility, their fabrication processes do not allow to pattern
 250 surface of the substrates in order to optimize the sensing area. Contrary to this, printing
 251 techniques are able to transfer different kind of layouts on the substrates, such as the capacitive
 252 structures presented in this work, which allows to enhance the sensitivity of humidity sensors
 253 more than two orders of magnitude. In addition, some of the presented processes are not suitable
 254 for a large-scale and cost-effective production of devices, as it is the case of the one presented
 255 in [49].

256 **Table 4.** Comparison with other biodegradable sensors.

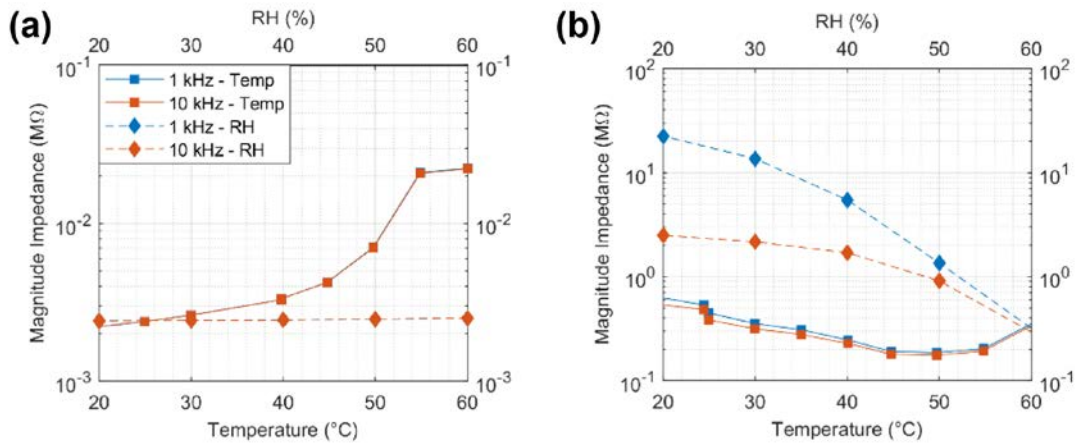
Reference	Sensor Type	Electrode and Substrate Materials	Fabrication Process	Area (cm ²)	Sensitivity ($\Delta Z /^\circ\text{C}$ or $\Delta Z /\%RH$)
Salvatore <i>et al.</i> [50]	Temperature	Mg/EcoFlex	UV lithography / etching	7	70 $\Omega/^\circ\text{C}$
Yi <i>et al.</i> [51]	Temperature	Zn/Galactomannan	Drop Casting	~0.5	5 $\Omega/^\circ\text{C}$
Liakos <i>et al.</i> [48]	Humidity	SWCNT, Sodium alginate, CaCl ₂	Immersion/Coating	-	1210 $\Omega/\%RH$ @ 1kHz
Zhu <i>et al.</i> [49]	Humidity	Cellulose Nanofibers, CNTs	Vacuum filtration	0.5	~1307 $\Omega/\%RH$ @ DC voltage
Syrový <i>et al.</i> [52]	Humidity	Carbon Paste Cellulose nanofibril	Screen-Printing	1	Up to 122 k $\Omega/\%RH$ @ 1kHz
Liu <i>et al.</i> [53]	Temperature	Laser-Induced Graphene (LIG)/Starch Film	Laser-Patterning and Transferring	-	~1.2 k $\Omega/^\circ\text{C}$
Barras <i>et al.</i> [54]	Humidity	Carbon Filaments and carboxymethyl cellulose on Paper	Screen-printing	0.7	~2.6 k $\Omega/\%RH$ @ DC voltage
This work	Humidity	PEDOT:PSS on Paper	Screen-Printing	4	217.2 k $\Omega/\%RH$ @ 1kHz
		PEDOT:PSS on PVA			207 k $\Omega/\%RH$ @ 1kHz
		Carbon Paste on Paper			204 k $\Omega/\%RH$ @ 1kHz

	PEDOT:PSS on Paper			25 $\Omega/^{\circ}\text{C}$ @ 10kHz
Temperature	Carbon Paste on Paper	Screen-Printing	1.5	75 $\Omega/^{\circ}\text{C}$

257
258 In the case of biodegradable temperature sensors, authors like Salvatore *et al.* [50] and Yi *et al.*
259 [51] also opted for the patterning of resistive layouts on biodegradable substrates; one of them
260 following a UV lithography and etching process, after which the pattern is transferred to the
261 substrate (which is a similar process to the one followed in the LIG-based sensor presented by
262 Liu *et al.* [53]); and the other following a mask-aided drop casting method. It can be seen that
263 the sensitivities of the temperature sensors presented in this work are higher than that obtained
264 with the Mg-based and Zn-based sensors, even with smaller areas (e.g., when compare the
265 carbon-based sensor with respect to the Mg-based one). Regarding printed sensors, although
266 there are numerous screen-printed as well as inkjet-printed sensors reported in the literature,
267 most of them are based on non-biodegradable materials (either the electrodes or even both
268 electrodes and substrates). Among the few fully biodegradable sensors that can be found are
269 the screen-printing approaches presented by Syrový *et al.* [52] and Barras *et al.* [54], which
270 demonstrate the trend towards the use of carbon materials on cellulose-based substrates for the
271 fabrication of fully biodegradable and printed sensors.

272
273 **3.5.Characterization as Hybrid Sensors**

274 Based on the results obtained for both RH and temperature sensors, the devices fabricated could
275 be successfully employed in a hybrid sensor, where the RH is extracted by measuring the
276 impedance between the terminals of IDE structure, and the temperature through one of the
277 junctions of the IDE structure, i.e., the line that links all fingers of one IDE terminal [55]. To
278 exemplify this concept, in Figure 7 we show a comparison between the impedance of a carbon-
279 based line of 3 mm of width and the impedance of a carbon-based IDE structure on the same
280 substrate (paper). These results show how at 1 kHz and 10 kHz the combination of the two
281 measurements, at the IDE terminals and at the line ends, would provide sufficient data to isolate
282 the effects of temperature and humidity, resulting in a biodegradable, compact, simple and cost-
283 effective multi-sensing method.



284

285 **Figure 7.** Impedance as a function of temperature and RH for a carbon-based line with 3 mm of width (a) and a carbon-based
 286 IDE structure (b), both on paper.

287

288 4. Conclusions

289 With this contribution, we intend to shift the focus of research in printed electronics and sensors
 290 towards a real sustainability of printed Internet of Things nodes. For this reason, we designed,
 291 fabricated and characterized a set of different sensors with biodegradable materials (both
 292 conductive materials and insulating substrates), in order to measure the temperature and
 293 humidity content in the environment. Our low-cost, sustainable and high throughput method
 294 allowed us to produce multi-sensing devices made of conductive polymers and a carbon-based
 295 paste on both paper and PVA substrates. The performances of these sensors are remarkable and
 296 detectable with low-cost equipment (0.04% change in relative resistance per degree Celsius, 1
 297 dec change in impedance per 20% RH). This factor, in combination with the facile production
 298 method and the significantly reduced environmental impact, makes this new class of sensors
 299 promising candidates for a sustainable development of sensors within the Internet of Everything
 300 paradigm.

301

302 Acknowledgements

303 This work was partially funded by the fellowship H2020-MSCA-IF-2017 794885-SELFSSENS,
 304 the TUM Graduate School and the Spanish Ministry of Education, Culture, and Sport through
 305 the predoctoral grant FPU16/01451.

306

- 308 [1] N. Wang, N. Zhang, and M. Wang, “Wireless sensors in agriculture and food industry—
309 Recent development and future perspective,” *Computers and Electronics in Agriculture*,
310 vol. 50, no. 1, pp. 1–14, Jan. 2006, doi: 10.1016/j.compag.2005.09.003.
- 311 [2] Z. Chen and C. Lu, “Humidity Sensors: A Review of Materials and Mechanisms,” Dec.
312 2005.
313 [https://www.ingentaconnect.com/content/asp/senlet/2005/00000003/00000004/art00002](https://www.ingentaconnect.com/content/asp/senlet/2005/00000003/00000004/art00002?token=006c1efa37b3d953bcdef68263c4a6f644a467c79675d7c4e4a47543c7e386f7e2a46762c20675d7d7067702e744a4553123b9853e5)
314 [?token=006c1efa37b3d953bcdef68263c4a6f644a467c79675d7c4e4a47543c7e386f7e2a](https://www.ingentaconnect.com/content/asp/senlet/2005/00000003/00000004/art00002?token=006c1efa37b3d953bcdef68263c4a6f644a467c79675d7c4e4a47543c7e386f7e2a46762c20675d7d7067702e744a4553123b9853e5)
315 [46762c20675d7d7067702e744a4553123b9853e5](https://www.ingentaconnect.com/content/asp/senlet/2005/00000003/00000004/art00002?token=006c1efa37b3d953bcdef68263c4a6f644a467c79675d7c4e4a47543c7e386f7e2a46762c20675d7d7067702e744a4553123b9853e5) (accessed Feb. 25, 2020).
- 316 [3] H. Farahani, R. Wagiran, and M. N. Hamidon, “Humidity Sensors Principle, Mechanism,
317 and Fabrication Technologies: A Comprehensive Review,” *Sensors*, vol. 14, no. 5, pp.
318 7881–7939, May 2014, doi: 10.3390/s140507881.
- 319 [4] F. A. Viola, A. Spanu, P. C. Ricci, A. Bonfiglio, and P. Cosseddu, “Ultrathin, flexible and
320 multimodal tactile sensors based on organic field-effect transistors,” *Scientific Reports*,
321 vol. 8, no. 1, Art. no. 1, May 2018, doi: 10.1038/s41598-018-26263-1.
- 322 [5] C. Liu *et al.*, “Highly stable pressure sensor based on carbonized melamine sponge using
323 fully wrapped conductive path for flexible electronic skin,” *Organic Electronics*, vol. 76,
324 p. 105447, Jan. 2020, doi: 10.1016/j.orgel.2019.105447.
- 325 [6] C. Rullyani, M. Ramesh, C.-F. Sung, H.-C. Lin, and C.-W. Chu, “Natural polymers for
326 disposable organic thin film transistors,” *Organic Electronics*, vol. 54, pp. 154–160, Mar.
327 2018, doi: 10.1016/j.orgel.2017.12.034.
- 328 [7] M. Irimia-Vladu, Eric. D. Głowacki, G. Voss, S. Bauer, and N. S. Sariciftci, “Green and
329 biodegradable electronics,” *Materials Today*, vol. 15, no. 7, pp. 340–346, Jul. 2012, doi:
330 10.1016/S1369-7021(12)70139-6.
- 331 [8] M. Berggren, D. Nilsson, and N. D. Robinson, “Organic materials for printed electronics,”
332 *Nature Materials*, vol. 6, no. 1, Art. no. 1, Jan. 2007, doi: 10.1038/nmat1817.
- 333 [9] Y. Seekaew, S. Lokavee, D. Phokharatkul, A. Wisitsoraat, T. Kerdcharoen, and C.
334 Wongchoosuk, “Low-cost and flexible printed graphene–PEDOT:PSS gas sensor for
335 ammonia detection,” *Organic Electronics*, vol. 15, no. 11, pp. 2971–2981, Nov. 2014, doi:
336 10.1016/j.orgel.2014.08.044.
- 337 [10] V. Dua *et al.*, “All-Organic Vapor Sensor Using Inkjet-Printed Reduced Graphene Oxide,”
338 *Angewandte Chemie International Edition*, vol. 49, no. 12, pp. 2154–2157, 2010, doi:
339 10.1002/anie.200905089.
- 340 [11] S. Lim, B. Kang, D. Kwak, W. H. Lee, J. A. Lim, and K. Cho, “Inkjet-Printed Reduced
341 Graphene Oxide/Poly(Vinyl Alcohol) Composite Electrodes for Flexible Transparent
342 Organic Field-Effect Transistors,” *J. Phys. Chem. C*, vol. 116, no. 13, pp. 7520–7525, Apr.
343 2012, doi: 10.1021/jp203441e.
- 344 [12] F. J. Romero, A. Rivadeneyra, M. Becherer, D. P. Morales, and N. Rodríguez,
345 “Fabrication and Characterization of Humidity Sensors Based on Graphene Oxide–
346 PEDOT:PSS Composites on a Flexible Substrate,” *Micromachines*, vol. 11, no. 2, Art. no.
347 2, Feb. 2020, doi: 10.3390/mi11020148.
- 348 [13] S. Miserere, S. Ledru, N. Ruillé, S. Griveau, M. Boujtita, and F. Bedioui, “Biocompatible
349 carbon-based screen-printed electrodes for the electrochemical detection of nitric oxide,”
350 *Electrochemistry Communications*, vol. 8, no. 2, pp. 238–244, Feb. 2006, doi:
351 10.1016/j.elecom.2005.11.016.
- 352 [14] X. Liu, M. Mwangi, X. Li, M. O’Brien, and G. M. Whitesides, “Paper-based piezoresistive
353 MEMS sensors,” *Lab Chip*, vol. 11, no. 13, pp. 2189–2196, Jun. 2011, doi:
354 10.1039/C1LC20161A.

- 355 [15] J. G. Bell, M. P. S. Mousavi, M. K. Abd El-Rahman, E. K. W. Tan, S. Homer-
356 Vanniasinkam, and G. M. Whitesides, "Paper-based potentiometric sensing of free
357 bilirubin in blood serum," *Biosensors and Bioelectronics*, vol. 126, pp. 115–121, Feb.
358 2019, doi: 10.1016/j.bios.2018.10.055.
- 359 [16] M. S. Verma *et al.*, "Sliding-strip microfluidic device enables ELISA on paper,"
360 *Biosensors and Bioelectronics*, vol. 99, pp. 77–84, Jan. 2018, doi:
361 10.1016/j.bios.2017.07.034.
- 362 [17] J. N. Palasagaram and R. Ramadoss, "MEMS-Capacitive Pressure Sensor Fabricated
363 Using Printed-Circuit-Processing Techniques," *IEEE Sensors Journal*, vol. 6, no. 6, pp.
364 1374–1375, Dec. 2006, doi: 10.1109/JSEN.2006.884430.
- 365 [18] G. DeJean, R. Bairavasubramanian, D. Thompson, G. E. Ponchak, M. M. Tentzeris, and
366 J. Papapolymerou, "Liquid Crystal polymer (LCP): a new organic material for the
367 development of multilayer dual-frequency/dual-polarization flexible antenna arrays,"
368 *IEEE Antennas and Wireless Propagation Letters*, vol. 4, pp. 22–26, 2005, doi:
369 10.1109/LAWP.2004.841626.
- 370 [19] Y. Okahisa, A. Yoshida, S. Miyaguchi, and H. Yano, "Optically transparent wood-
371 cellulose nanocomposite as a base substrate for flexible organic light-emitting diode
372 displays," *Composites Science and Technology*, vol. 69, no. 11, pp. 1958–1961, Sep. 2009,
373 doi: 10.1016/j.compscitech.2009.04.017.
- 374 [20] J. Xu *et al.*, "Conductive polypyrrole-bacterial cellulose nanocomposite membranes as
375 flexible supercapacitor electrode," *Organic Electronics*, vol. 14, no. 12, pp. 3331–3338,
376 Dec. 2013, doi: 10.1016/j.orgel.2013.09.042.
- 377 [21] M. U. Khan, Q. M. Saqib, G. Hassan, and J. Bae, "All printed organic humidity sensor
378 based on egg albumin," *Sensing and Bio-Sensing Research*, vol. 28, p. 100337, Jun. 2020,
379 doi: 10.1016/j.sbsr.2020.100337.
- 380 [22] S. Hajian *et al.*, "Development of a Fluorinated Graphene-Based Resistive Humidity
381 Sensor," *IEEE Sensors Journal*, vol. 20, no. 14, pp. 7517–7524, Jul. 2020, doi:
382 10.1109/JSEN.2020.2985055.
- 383 [23] X. Zhang *et al.*, "Printed Carbon Nanotubes-Based Flexible Resistive Humidity Sensor,"
384 *IEEE Sensors Journal*, vol. 20, no. 21, pp. 12592–12601, Nov. 2020, doi:
385 10.1109/JSEN.2020.3002951.
- 386 [24] V. S. Turkani *et al.*, "A highly sensitive printed humidity sensor based on a functionalized
387 MWCNT/HEC composite for flexible electronics application," *Nanoscale Adv.*, vol. 1, no.
388 6, pp. 2311–2322, Jun. 2019, doi: 10.1039/C9NA00179D.
- 389 [25] R. Alrammouz *et al.*, "Highly porous and flexible capacitive humidity sensor based on
390 self-assembled graphene oxide sheets on a paper substrate," *Sensors and Actuators B:
391 Chemical*, vol. 298, p. 126892, Nov. 2019, doi: 10.1016/j.snb.2019.126892.
- 392 [26] F. Güder *et al.*, "Paper-Based Electrical Respiration Sensor," *Angewandte Chemie
393 International Edition*, vol. 55, no. 19, pp. 5727–5732, 2016, doi: 10.1002/anie.201511805.
- 394 [27] S. Kanaparthi, "Pencil-drawn Paper-based Non-invasive and Wearable Capacitive
395 Respiration Sensor," *Electroanalysis*, vol. 29, no. 12, pp. 2680–2684, 2017, doi:
396 10.1002/elan.201700438.
- 397 [28] Z. Duan *et al.*, "Facile, Flexible, Cost-Saving, and Environment-Friendly Paper-Based
398 Humidity Sensor for Multifunctional Applications," *ACS Appl. Mater. Interfaces*, vol. 11,
399 no. 24, pp. 21840–21849, Jun. 2019, doi: 10.1021/acsami.9b05709.
- 400 [29] Z. Ahmad, M. Abbas, I. Gunawan, R. A. Shakoar, F. Ubaid, and F. Touati, "Electro-
401 sprayed PVA coating with texture-enriched surface morphology for augmented humidity
402 sensing," *Progress in Organic Coatings*, vol. 117, pp. 7–9, Apr. 2018, doi:
403 10.1016/j.porgcoat.2017.12.010.

- 404 [30] AGFA, “ORGACONTM conductive polymer screen-printing inks.” Sep. 26, 2018,
405 Accessed: Nov. 19, 2020. [Online]. Available: [https://www.agfa.com/specialty-](https://www.agfa.com/specialty-products/wp-content/uploads/sites/8/2018/10/Screen-Printing-inks-2018v4.0.pdf)
406 [products/wp-content/uploads/sites/8/2018/10/Screen-Printing-inks-2018v4.0.pdf](https://www.agfa.com/specialty-products/wp-content/uploads/sites/8/2018/10/Screen-Printing-inks-2018v4.0.pdf).
- 407 [31] Henkel, “LOCTITE ECI 8001 E&C - Technical Data Sheet.” 2017, [Online]. Available:
408 [https://dm.henkel-dam.com/is/content/henkel/lt-5980-brochure-printed-electronics-inks-](https://dm.henkel-dam.com/is/content/henkel/lt-5980-brochure-printed-electronics-inks-and-coatings)
409 [and-coatings](https://dm.henkel-dam.com/is/content/henkel/lt-5980-brochure-printed-electronics-inks-and-coatings).
- 410 [32] I. Moutinho, P. Oliveira, M. Figueiredo, and P. Ferreira, “EVALUATING THE
411 SURFACE ENERGY OF SURFACE SIZED PRINTING AND WRITING PAPERS,”
412 2007. /paper/EVALUATING-THE-SURFACE-ENERGY-OF-SURFACE-SIZED-AND-
413 Moutinho-Oliveira/28fbc81c4a81cf2ad545e3434d55cba27214c526 (accessed Nov. 19,
414 2020).
- 415 [33] DuPont Teijin Films, “MELINEX® ST506.” Mar. 24, 2016, Accessed: Nov. 19, 2020.
416 [Online]. Available: [https://usa.dupontteijinfilms.com/wp-](https://usa.dupontteijinfilms.com/wp-content/uploads/2017/01/ST506-Datasheet.pdf)
417 [content/uploads/2017/01/ST506-Datasheet.pdf](https://usa.dupontteijinfilms.com/wp-content/uploads/2017/01/ST506-Datasheet.pdf).
- 418 [34] F. J. Romero *et al.*, “Design, fabrication and characterization of capacitive humidity
419 sensors based on emerging flexible technologies,” *Sensors and Actuators B: Chemical*,
420 vol. 287, pp. 459–467, May 2019, doi: 10.1016/j.snb.2019.02.043.
- 421 [35] A. Rivadeneyra, J. Fernández-Salmerón, J. Banqueri, J. A. López-Villanueva, L. F.
422 Capitan-Vallvey, and A. J. Palma, “A novel electrode structure compared with
423 interdigitated electrodes as capacitive sensor,” *Sensors and Actuators B: Chemical*, vol.
424 204, pp. 552–560, Dec. 2014, doi: 10.1016/j.snb.2014.08.010.
- 425 [36] A. Rivadeneyra *et al.*, “Cost-Effective PEDOT:PSS Temperature Sensors Inkjetted on a
426 Bendable Substrate by a Consumer Printer,” *Polymers*, vol. 11, no. 5, Art. no. 5, May 2019,
427 doi: 10.3390/polym11050824.
- 428 [37] X. He *et al.*, “Hexagonal and Square Patterned Silver Nanowires/PEDOT:PSS Composite
429 Grids by Screen Printing for Uniformly Transparent Heaters,” *Polymers*, vol. 11, no. 3,
430 Art. no. 3, Mar. 2019, doi: 10.3390/polym11030468.
- 431 [38] S. K. M. Jönsson *et al.*, “The effects of solvents on the morphology and sheet resistance
432 in poly(3,4-ethylenedioxythiophene)–polystyrenesulfonic acid (PEDOT–PSS) films,”
433 *Synthetic Metals*, vol. 139, no. 1, pp. 1–10, Aug. 2003, doi: 10.1016/S0379-
434 6779(02)01259-6.
- 435 [39] A. Denneulin, A. Blayo, J. Bras, and C. Neuman, “PEDOT:PSS coating on specialty
436 papers: Process optimization and effects of surface properties on electrical performances,”
437 *Progress in Organic Coatings*, vol. 63, no. 1, pp. 87–91, Jul. 2008, doi:
438 10.1016/j.porgcoat.2008.04.009.
- 439 [40] P. Wilson, C. Lekakou, and J. F. Watts, “A comparative assessment of surface
440 microstructure and electrical conductivity dependence on co-solvent addition in spin
441 coated and inkjet printed poly(3,4-ethylenedioxythiophene):polystyrene sulphonate
442 (PEDOT:PSS),” *Organic Electronics*, vol. 13, no. 3, pp. 409–418, Mar. 2012, doi:
443 10.1016/j.orgel.2011.11.011.
- 444 [41] A. Albrecht, J. F. Salmeron, M. Becherer, P. Lugli, and A. Rivadeneyra, “Screen-Printed
445 Chipless Wireless Temperature Sensor,” *IEEE Sensors Journal*, vol. 19, no. 24, pp.
446 12011–12015, Dec. 2019, doi: 10.1109/JSEN.2019.2940836.
- 447 [42] J. Mamouni and L. Yang, “Interdigitated microelectrode-based microchip for electrical
448 impedance spectroscopic study of oral cancer cells,” *Biomed Microdevices*, vol. 13, no. 6,
449 pp. 1075–1088, Dec. 2011, doi: 10.1007/s10544-011-9577-8.
- 450 [43] Y. Feng, J. Hallstedt, Q. Chen, L.-R. Zheng, and Y. Huang, “Development and
451 experimental verification of analytical models for printable interdigital capacitor sensors
452 on paperboard,” in *2009 IEEE SENSORS*, Oct. 2009, pp. 1034–1039, doi:
453 10.1109/ICSENS.2009.5398531.

- 454 [44] Y. Zhang and Y. Cui, "Development of Flexible and Wearable Temperature Sensors
455 Based on PEDOT:PSS," *IEEE Transactions on Electron Devices*, vol. 66, no. 7, pp. 3129–
456 3133, Jul. 2019, doi: 10.1109/TED.2019.2914301.
- 457 [45] W. Honda, S. Harada, T. Arie, S. Akita, and K. Takei, "Printed wearable temperature
458 sensor for health monitoring," in *2014 IEEE SENSORS*, Nov. 2014, pp. 2227–2229, doi:
459 10.1109/ICSENS.2014.6985483.
- 460 [46] J. Maslik, H. Andersson, V. Forsberg, M. Engholm, R. Zhang, and H. Olin, "PEDOT:PSS
461 temperature sensor ink-jet printed on paper substrate," *J. Inst.*, vol. 13, no. 12, pp.
462 C12010–C12010, Dec. 2018, doi: 10.1088/1748-0221/13/12/C12010.
- 463 [47] M. Yang and M. Zhang, "Biodegradation of Carbon Nanotubes by Macrophages," *Front.*
464 *Mater.*, vol. 6, 2019, doi: 10.3389/fmats.2019.00225.
- 465 [48] I. L. Liakos, A. Mondini, C. Filippeschi, V. Mattoli, F. Tramacere, and B. Mazzolai,
466 "Towards ultra-responsive biodegradable polysaccharide humidity sensors," *Materials*
467 *Today Chemistry*, vol. 6, pp. 1–12, Dec. 2017, doi: 10.1016/j.mtchem.2017.08.001.
- 468 [49] P. Zhu *et al.*, "Flexible and Highly Sensitive Humidity Sensor Based on Cellulose
469 Nanofibers and Carbon Nanotube Composite Film," *Langmuir*, vol. 35, no. 14, pp. 4834–
470 4842, Apr. 2019, doi: 10.1021/acs.langmuir.8b04259.
- 471 [50] G. A. Salvatore *et al.*, "Biodegradable and Highly Deformable Temperature Sensors for
472 the Internet of Things," *Advanced Functional Materials*, vol. 27, no. 35, p. 1702390, 2017,
473 doi: 10.1002/adfm.201702390.
- 474 [51] N. Yi *et al.*, "Fully Water-Soluble, High-Performance Transient Sensors on a Versatile
475 Galactomannan Substrate Derived from the Endosperm," *ACS Appl. Mater. Interfaces*,
476 vol. 10, no. 43, pp. 36664–36674, Oct. 2018, doi: 10.1021/acsami.8b11682.
- 477 [52] T. Syrový *et al.*, "Wide range humidity sensors printed on biocomposite films of cellulose
478 nanofibril and poly(ethylene glycol)," *Journal of Applied Polymer Science*, vol. 136, no.
479 36, p. 47920, 2019, doi: <https://doi.org/10.1002/app.47920>.
- 480 [53] H. Liu *et al.*, "Flexible and Degradable Multimodal Sensor Fabricated by Transferring
481 Laser-Induced Porous Carbon on Starch Film," *ACS Sustainable Chem. Eng.*, vol. 8, no.
482 1, pp. 527–533, Jan. 2020, doi: 10.1021/acssuschemeng.9b05968.
- 483 [54] R. Barras, I. Cunha, D. Gaspar, E. Fortunato, R. Martins, and L. Pereira, "Printable
484 cellulose-based electroconductive composites for sensing elements in paper electronics,"
485 *Flex. Print. Electron.*, vol. 2, no. 1, p. 014006, Mar. 2017, doi: 10.1088/2058-8585/aa5ef9.
- 486 [55] A. Rivadeneyra, J. Fernández-Salmerón, M. Agudo-Acemel, J. A. López-Villanueva, L.
487 F. Capitán-Vallvey, and A. J. Palma, "Hybrid Printed Device for Simultaneous Vapors
488 Sensing," *IEEE Sensors Journal*, vol. 16, no. 23, pp. 8501–8508, Dec. 2016, doi:
489 10.1109/JSEN.2016.2606415.

491

492 **Fabrication and characterization of fully printed biodegradable sensors for humidity and**
493 **temperature sensing. These sensors will contribute enormously to pave the way to more**
494 **cost-effective and environmental friendly devices.**

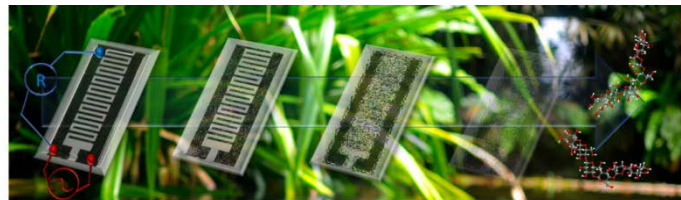
495 **Keywords: carbon; humidity; paper; PVA; PEDOT:PSS; screen-printing; temperature**

496 *Aniello Falco, Philipp S. Sackenheim, Francisco J. Romero, Markus Becherer, Paolo Lugli,*
497 *José F. Salmeron, Almudena Rivadeneyra**

498 **Fabrication of low cost and low impact RH and temperature sensors, for the Internet of**
499 **Environmental-Friendly Things**

500

501



502

503

504

505